To: **International Journal of Hydrogen Energy**

Transport Properties of Acceptor-Doped Barium Zirconate by Electromotive Force Measurements

Donglin Han [a, *], Yohei Noda [a, b], Takayuki Onishi [a], Naoyuki Hatada [a], Masatoshi Majima [b] and Tetsuya Uda [a, *]

[a] Department of Materials Science and Engineering, Kyoto University,

Yoshida Honmachi, Sakyo-ku, Kyoto 606-8501, Japan

[b] Sumitomo Electric Industries, Ltd.,

1-1-1, Koyakita, Itami-shi, Hyogo 664-0016, Japan

* Corresponding authors: Donglin Han (han.donglin.8n@kyoto-u.ac.jp)

and Tetsuya Uda (uda_lab@aqua.mtl.kyoto-u.ac.jp)

TEL: +81-75-753-5445, FAX: +81-75-753-5284

Abstract

In this work, a systematic work was performed to investigate the electrochemical transport properties of acceptor-doped $BaZrO_3$ by measuring electromotive force on various gas concentration cells. For the measurements in the wet oxidizing atmosphere, where significant hole conduction occurs, the transport numbers of the ionic conduction in the oxidizing atmosphere were corrected by taking the effect of electrode polarization into consideration. The results revealed that regardless of whether Sc, Y, In, Ho, Er, Tm or Yb was doped, proton conduction predominates in the reducing atmosphere with the transport number close to unit. However, the contribution of ionic conduction weakens, and the contribution of hole conduction enhances, when the samples are exposed to the moist oxidizing atmosphere. In addition, introducing Ba-deficiency results in degraded electrochemical conductivity, but the transport number in either the moist reducing or the moist oxidizing atmosphere does not change obviously.

Key words: Barium zirconate; Ba-deficiency; transport number; proton conduction; fuel cell

1. Introduction

Proton conductive acceptor-doped barium zirconate ($BaZrO_3$) is promising as an electrolyte in electrochemical devices, such as fuel cells [1-3] and electrolysis cells [4]. In addition to some other important properties like chemical stability against reaction with CO_2, the most vital one is its special transport properties in humid reducing atmosphere; that is, quite pure proton conduction (the transport number is close to unity [5, 6]), and high value of conductivity (> 0.01 Scm^{-1} at 600 ^oC [7-9]). But, the transport property of the acceptor-doped $BaZrO_3$ changed with variation of oxygen potential in environmental atmosphere. Taking Y-doped $BaZrO_3$ (BZY) for example, conduction of electronic holes is enhanced significantly in a pure oxygen atmosphere [6]. Since in most cases during the fuel cell operation, cathode side is exposed to the atmosphere with high oxygen potential, the hole conduction thereby generated might influence the performance of the fuel cells negatively, such as by lowering the open circuit voltage. [10]

There are several works on the transport property of BZY in oxidizing atmosphere. Schober and Bohn [5] applied electromotive force (EMF) method on gas concentration cells with $BaZr_{0.9}Y_{0.1}O_{3-\delta}$ as the electrolyte, and found that the transport number of protons (t_{H^+}) conduction is not higher than 0.03 in a wet oxidizing atmosphere at temperatures ranging from 400 to 800 ^oC. Lately, studies by analyzing the dependence of conductivity on oxygen partial pressure lead to a different conclusion [6, 11]. In the oxidizing atmosphere, Wang and Virkar [11] reported t_{H^+} > 0.5 for $BaZr_{0.93}Y_{0.07}O_{3-\delta}$ at 500 ^oC, and Nomura and Kageyama [6] reported a sum of the transport numbers of proton and oxide

ion conduction to be about 0.4 for $BaZr_{0.8}Y_{0.2}O_{3-\delta}$ at 600 ºC. And a similar conclusion was generated in a recent work by Kim, *et al*. using conductivity relaxation method to study the transport property of $BaZr_{0.8}Y_{0.2}O_{3-\delta}$ [12]. Transport numbers are practically important properties for electrochemical devices, and we need to discuss the reason for such controversy in literatures, and determine true values. In addition, Ho, Er, Tm and Yb were found to impart $BaZrO_3$ with high proton conductivity comparable with that of BZY [8, 13, 14]. Therefore, a detailed study on the transport property of the samples doped with Ho, Er, Tm and Yb seems to be necessary and important.

In this work, the electromotive force method was applied to investigate the transport property of stoichiometric and Ba-deficient BZY, and also $BaZrO_3$ doped with 20 mol% Ho, Er, Tm, Yb, Sc and In. Based on the results thereby obtained, dependence of transport properties on the Ba-deficiency and dopants was discussed.

2. Experimental

2.1 Material preparation

Samples with the nominal composition of $BaZr_{0.8}M_{0.2}O_{3-\delta}$ (M =Sc, Y, In, Ho, Er, Tm and Yb), $BaZr_{0.9}Y_{0.1}O_{3-\delta}$, and $Ba_{1-x}Zr_{0.8}Y_{0.2}O_{3-\delta}$ (x = 0.02 and 0.05) were prepared by a conventional solid state reaction method. Starting materials of $BaCO_3$ (Wako Pure Chemical Industries, Ltd., 99.9%), ZrO_2 (Tosoh Corporation, 98.01%), and Sc_2O_3 (Daiichi Kigenso Kagaku Kogyo Co., Ltd., 99.99%), Y_2O_3 (Shin-Etsu Chemical Co., Ltd., 99.9%), In_2O_3 (Nacalai Tesque Inc., 99.9%), Ho_2O_3 (Sigma-Aldrich

Chemie GmbH, 99.9%), Er_2O_3 (Wako Pure Chemical Industries, Ltd., 99.9%), Tm_2O_3 (Wako Pure Chemical Industries, Ltd., 99.9%) or Yb_2O_3 (Shin-Etsu Chemical Co., Ltd., 99.9%) were mixed at the desired ratios, and ball-milled for 24 h. Mixtures were then pelletized under 9.8 MPa and heat-treated at 1000 ^oC in ambient atmosphere for 10 h. After ball-milling for 10 h, the samples were pelletized under 9.8 MPa again, and kept at 1300 ^oC for 10 h in ambient atmosphere for synthesizing. The samples were then ball-milled for 100 h, and subsequently mixed with a binder (NCB-166, DIC Corporation, Tokyo, Japan). The mixtures were then pelletized at 392 MPa, and heat-treated at 600 ^oC for 8 h to remove the binder. The thereby prepared pellet-like samples of $Ba_{1-x}Zr_{0.8}Y_{0.2}O_{3-\delta}$ (x = 0.02 and 0.05) were buried in their relevant synthesized powder, and the other samples were buried in mixtures of the relevant synthesized powders (99 wt%) and $BaCO_3$ (1 wt%). Finally, all the samples were heated at 1600 ^oC for 24 h in pure oxygen atmosphere for sintering.

2.2 Characterization

X-ray diffraction (XRD) measurements were performed on powder samples at room temperature using Cu $K\alpha$ radiation with X'Pert-ProMPD (PANalytical, Almelo, Netherland). Rietveld refinement was performed to determine lattice constants with a commercial software X'Pert HighScore Plus. Chemical compositions were determined by inductively coupled plasma atomic emission spectroscopy (ICP-AES) with SPS3500 (Seiko Instruments Inc., Chiba, Japan). Microstructures were observed by scanning electron microscopy (SEM) with VE-7800 (Keyence Co., Osaka, Japan). Conductivities of

the as-sintered pellet-like samples of $Ba_{1-x}Zr_{0.8}Y_{0.2}O_{3-\delta}$ (x = 0.02 and 0.05) with sputtered platinum (Pt) electrodes were measured in a wet atmosphere of O_2 or H_2. Water partial pressure in these wet atmospheres was kept at 0.05 atm by bubbling through deionized water kept at 33 ºC. Impedance spectra were collected by A. C. impedance spectroscopy in the frequency range from 10 Hz to 7 MHz using a frequency response analyzer (Solartron SI 1260, Solartron Analytical, UK) with an applied A. C. voltage of 100 mV at temperatures ranging from 600 to 100 ºC.

2.3 Theoretical Considerations

2.3.1 EMF Methods

It is a conventional method to determine the transport numbers of different charge carriers by measuring EMFs of gas concentration cells [15 - 21] with a brief structure as:

gas(I), electrode(I) | electrolyte | electrode(II), gas(II)

In acceptor-doped $BaZrO_3$, protons, oxide ions, holes and electrons are candidate charge carriers. Theoretical EMFs (V_{cal}) generated due to the gradient in inner potential and chemical potential of the ionic charge carriers (protons and oxide ions) can be calculated through Eq. (1) [15, 19] (derivation is given in supplemental material), in which R is the ideal gas constant, F the Faraday constant, T the temperature, t the transport number, and p the partial pressure of gas specie (H_2, O_2 or H_2O) at the corresponding electrode marked with superscripts of I or II.

$$V_{\text{cal}} = t_{\text{H}^+} \frac{\text{R}T}{2\text{F}} \ln\left(\frac{p^{\text{I}}_{\text{H}_2}}{p^{\text{II}}_{\text{H}_2}}\right) + t_{\text{O}^{2-}} \frac{\text{R}T}{4\text{F}} \ln\left(\frac{p^{\text{II}}_{\text{O}_2}}{p^{\text{I}}_{\text{O}_2}}\right) \quad (1)$$

Taking the equilibrium of reaction (Eq. (2)) into consideration, Eq. (1) can be rewritten as Eq. (3) and (4).

$$2\text{H}_2 + \text{O}_2 = 2\text{H}_2\text{O} \quad (2)$$

$$V_{\text{cal}} = (t_{\text{H}^+} + t_{\text{O}^{2-}}) \frac{\text{R}T}{2\text{F}} \ln\left(\frac{p^{\text{I}}_{\text{H}_2}}{p^{\text{II}}_{\text{H}_2}}\right) + t_{\text{O}^{2-}} \frac{\text{R}T}{2\text{F}} \ln\left(\frac{p^{\text{II}}_{\text{H}_2\text{O}}}{p^{\text{I}}_{\text{H}_2\text{O}}}\right) \quad (3)$$

$$V_{\text{cal}} = (t_{\text{H}^+} + t_{\text{O}^{2-}}) \frac{\text{R}T}{4\text{F}} \ln\left(\frac{p^{\text{II}}_{\text{O}_2}}{p^{\text{I}}_{\text{O}_2}}\right) + t_{\text{H}^+} \frac{\text{R}T}{2\text{F}} \ln\left(\frac{p^{\text{I}}_{\text{H}_2\text{O}}}{p^{\text{II}}_{\text{H}_2\text{O}}}\right) \quad (4)$$

By carefully selecting the gas components fed to the two electrodes (details will be described in 2.4), the transport numbers (t_i) of the correspondent ionic species i can be determined by dividing the measured EMFs (V_{mea}) with the theoretical values (Eq. (5)), which are calculated under the assumption that the sum of the transport numbers of ionic species is unit, as shown in Eq. (5).

$$t_i = \frac{V_{\text{mea}}}{V_{\text{cal}}} \quad (5)$$

2.3.2 Reasonability to Treat Transport Number as Constant

For applying Eq. (1) to (5), one important assumption has to be made is that the transport numbers of the ionic species are constant across the electrolyte whose two surfaces are exposed to different atmospheres. But actually, in the acceptor-doped $BaZrO_3$, according to Eq. (6), the contribution of hole conduction is enhanced with the increasing partial pressure of oxygen (p_{O_2}) [6]. In addition, from Eq. (6), one can see that with the increasing p_{O_2}, the concentration of oxide ion vacancies ($\text{V}_{\text{O}}^{\bullet\bullet}$)

decreases with the increasing p_{O_2}, but such decrease is not so significant compared with the existing amount of $V_O^{\bullet\bullet}$ [22]. And in general, the total conductivity (σ_{total}) can be described using Eq. (7), where σ_{ion} is the ionic conduction which does not show strong dependence on p_{O_2}, and σ_h is the hole conductivity at p_{O_2} = 1 atm [6, 23, 24]. The transport number of ionic species (t_{ion}) can be consequently calculated using Eq. (8). Here, by simulating Eq. (8) with t_{ion} at p_{O_2} = 1 atm varying from 0.1 to 0.9 with an interval of 0.1, we obtained **Fig. 1**. Definitely, one can see that t_{ion} increased with the decreasing p_{O_2}. But, when the difference in p_{O_2} is small, the difference in t_{ion} is not large. For example, the difference in t_{ion} between p_{O_2} of 0.3 and 1 atm is typically less than 0.05 and not higher than 0.08.

$$2V_O^{\bullet\bullet} + O_2 = 2O_O^{\times} + 4h^{\bullet} \tag{6}$$

$$\sigma_{total} = \sigma_{ion} + \sigma_h (p_{O_2})^{\frac{1}{4}} \tag{7}$$

$$t_{ion} = \frac{\sigma_{ion}}{\sigma_{ion} + \sigma_h (p_{O_2})^{\frac{1}{4}}} \tag{8}$$

2.3.3 Correction by Considering Electrode Polarization

Another important thing has to be stressed here is that in a mixed conducting system where both the ionic and electronic conduction is significant, simply adopting Eq. (5) introduces underestimation of the contribution of the ionic conduction. [25-29] It is necessary to take the electrode polarization into consideration. And the ionic transport numbers can be corrected using Eq. (9) [25, 26], in which $R_{electrolyte}$ is the resistance of the electrolyte, R_{total} is the resistance of the whole cell composed of

$R_{electrolyte}$ and the polarization resistance of electrode.

$$t_i = 1 - \frac{R_{electrolyte}}{R_{total}}\left(1 - \frac{V_{mea}}{V_{cal}}\right) \quad (9)$$

2.4 Structure of Gas Concentration Cells for EMF Measurements

In this work, four different kinds of gas concentration cells were prepared as followings:

(Cell 1) Hydrogen concentration cell:

H_2 – 3.12% H_2O, Pt electrode (I) | Electrolyte | Pt electrode (II), Ar – H_2 – 3.12% H_2O

The H_2 partial pressure (p_{H_2}) at Pt electrode (I) is kept unvaried. And p_{H_2} at Pt electrode (II) changed by diluting with Ar. Since water vapor was fed to the two electrodes at an identical partial pressure (p_{H_2O}) of 0.0312 atm by bubbling through deionized water kept at 25 ^oC, according to Eq. (3), the sum of the transport numbers of proton and oxide ion conductions in H_2-contained reducing atmosphere can be determined.

(Cell 2) Water vapor (in hydrogen) concentration cell:

Ar – 19.83% H_2 – 0.86% H_2O, Pt electrode (I) | Electrolyte | Pt electrode (II), Ar – 19.38% H_2 – 3.12% H_2O

The transport number of oxide ion conduction ($t_{O^{2-}}$) in the H_2-contained reducing atmosphere can be determined according to Eq. (3), by supplying the gases with the same p_{H_2}, but different p_{H_2O} to the two electrodes. However, restricted by the precision on gas mixing, it was only available for us to bubble H_2 – 80% Ar gas through deionized water, which was kept at 5 and 25 ^oC for electrodes (I)

and (II), respectively, resulting in a difference in the p_{H_2}. Neglecting such difference results in underestimation of $t_{O^{2-}}$ (about 0.018 in maximum at 600 °C). However, such underestimation is too small to expect a significant influence.

(Cell 3) Oxygen concentration cell:

O_2 – Ar - 3.12% H_2O, Pt electrode (I) | Electrolyte | Pt electrode (II), O_2 - 3.12% H_2O

The O_2 partial pressure (p_{O_2}) was kept unvaried at Pt electrode (II), but was controlled by mixing with Ar to obtain appropriate value at Pt electrode (I). The same p_{H_2O} of 0.312 atm was fed to both the two electrodes. The sum of the transport numbers of proton and oxide ion conduction in O_2-contained oxidizing atmosphere can be determined by Eq. (4).

(Cell 4) Water vapor (in oxygen) concentration cell:

Ar – 19.38% O_2 - 3.12% H_2O, Pt electrode (I) | Electrolyte | Pt electrode (II), Ar – 19.83% O_2 – 0.86% H_2O

According to Eq. (4), transport number of the proton conduction (t_{H^+}) in the O_2-contained oxidizing atmosphere can be determined with Cell 4. But, similar to the case of Cell 2, a mixed gas of O_2 – 80% Ar was bubbled through deionized water here. And a small difference in p_{O_2} between the atmospheres for two electrodes results in generation of EMF (about 0.43 mV in maximum at 600 °C), and an underestimation of the transport number (about 0.009 at 600 °C). But, it is reasonable to neglect the influence of such value, since it is too small.

For all these four types of cells, pellet-like electrolytes sintered at 1600 °C with two opposite surfaces

sputtered with Pt electrodes were used. The thickness and diameter of the electrolytes were about 1 mm and 9 mm, respectively. Then, the samples were sealed into alumina holders using zirconia cement, as shown in **Fig. 2**, and were subsequently set into a home-made device. In such device, gases with different compositions were fed to the two electrodes. The temperature was kept at 500, 600 or 700 ^{o}C. EMFs thereby generated were recorded with Solartron 1287 (Solartron Analytical, Farnborough, UK). In order to eliminate the effect of thermovoltage, gases fed to the two electrodes were swapped, and an average value of EMFs recorded with direct and reverse gas feeding was adopted to determine the transport number (an example is given in **Fig. S1**). [21, 28, 29]

3. Results

3.1 Phase Identification and Composition Analysis

Total compositions determined by ICP-AES of stoichiometric $BaZr_{0.9}Y_{0.1}O_{3-\delta}$ and $BaZr_{0.8}Y_{0.2}O_{3-\delta}$, and Ba-deficient samples of $Ba_{0.98}Zr_{0.8}Y_{0.2}O_{3-\delta}$ and $Ba_{0.95}Zr_{0.8}Y_{0.2}O_{3-\delta}$ are given in **Table 1**, and are close to the nominal values. XRD patterns shown in **Fig. 3** indicates that only diffraction peaks belonging to single perovskite phases are observed for all these samples. The lattice constants of $BaZr_{0.8}Y_{0.2}O_{3-\delta}$, $Ba_{0.98}Zr_{0.8}Y_{0.2}O_{3-\delta}$ and $Ba_{0.95}Zr_{0.8}Y_{0.2}O_{3-\delta}$ determined by Rietveld refinement are 4.2371, 4.2265 and 4.2209 Å, respectively, indicating that the lattice shrinks with an increasing Ba-deficiency. In addition, as shown in **Fig. 4**, smaller grain size was obtained with larger Ba-deficiency. These results agree well with the literatures [30, 31].

The samples doped with 20 mol% Sc, In, Ho, Er, Tm and Yb were prepared with the same method as reported in our previous work. Single perovskite phases with the compositions close to the nominal values were obtained [8, 32].

3.2 Transport Properties of Stoichiometric Y-Doped $BaZrO_3$

3.2.1 EMF Method without Correction with Electrode Polarization

Firstly, transport properties of the stoichiometric samples of $BaZr_{0.9}Y_{0.1}O_{3-\delta}$ and $BaZr_{0.8}Y_{0.2}O_{3-\delta}$ were studied. As shown in **Fig. 5**, in the mode of hydrogen concentration cell, the measured EMF values are very close to the theoretical ones calculated based on an assumption of a pure ionic conduction ($t_{O^{2-}} + t_{H^+} = 1$) at 500, 600 and 700 ^oC. Such result indicates that the stoichiometric BZY exhibits almost pure ionic conduction in the reducing atmosphere. In the mode of water vapor (in hydrogen) concentration cell, as shown in **Fig. 6**, the measured EMFs are greatly lower than the theoretical values ($t_{O^{2-}} = 1$) at 500, 600 and 700 ^oC, indicating that the conduction of oxide ions in BZY is very minor in the humid reducing atmosphere.

Referring to measurements of oxygen concentration cells and water vapor (in oxygen) concentration cells, as shown in **Fig. 7** and **Fig. 8**, the measured values are greatly lower than the theoretical ones. It means that in addition to the conduction of ionic species, significant hole conduction generates when BZY is exposed to the oxidizing atmosphere.

Then, the transport numbers were estimated by dividing the measured EMFs value with the theoretical

ones (Eq. (5)), and are shown in **Fig. 9**. In the cases using a hydrogen or oxygen concentration cell, the transport numbers of the ionic conduction ($t_{O^{2-}} + t_{H^+}$) were obtained by linearly fitting the values calculated at various partial pressures of hydrogen (at electrode (II)) or oxygen (at electrode (I)) (an example is given in **Fig. S2**). [5, 20] It is worth to note that as shown in **Fig. 9(b)**, the transport numbers of the ionic conduction in $BaZr_{0.8}Y_{0.2}O_{3-\delta}$ in the wet oxidizing atmosphere (noted as "uncorrected"), where significant hole conduction is generated, are all less than 0.1. Such results agree with that reported by Schober and Bohn [5], but are greatly smaller than the other reports [6, 11].

3.2.2 Dependence of Total Conductivity on Partial Pressure of Oxygen

In order to check whether the results obtained in 3.2.1 are reasonable, dependence of total conductivity (σ_{total}) on p_{O_2} in the atmosphere was studied. The desired value of p_{O_2} was obtained by diluting O_2 or H_2 with Ar. And the partial pressure of water vapor was kept at 0.05 atm. As shown in **Fig. 10**, in the very low p_{O_2} (< 10^{-21} atm) area, σ_{total} almost kept constant regardless of variation of p_{O_2}, implying that there is hardly any electron conduction in such low p_{O_2} environment. However, in the high p_{O_2} (> 10^{-5} atm) area, σ_{total} increased with the increasing p_{O_2}, indicating that the contribution of hole conduction is enhanced with the increasing p_{O_2}. Then, the variation of σ_{total} with p_{O_2} was fitted using Eq. (7). The values of t_{ion} in wet O_2 (p_{H_2O} = 0.05 atm) thereby determined are 0.76, 0.36, 0.20 for $BaZr_{0.9}Y_{0.1}O_{3-\delta}$, and 0.89, 0.45, 0.23 for $BaZr_{0.8}Y_{0.2}O_{3-\delta}$ at 500, 600 and 700 ^{o}C, respectively. All the values are greatly larger than those determined by the EMF method

described in 3.2.1.

3.2.3 EMF Method Corrected with Electrode Polarization

The transport numbers of ionic conduction in oxidizing atmosphere obtained by the EMF method and by the relationship between σ_{total} and p_{O_2} are different apparently, but they should be consistent with each other. We then tried to take the effect of the electrode polarization (Eq. (6)) into consideration to correct the transport numbers determined by the EMF method [25, 26]. First of all, information of $R_{electrolyte}$ and R_{total} is necessary. The Solartron 1260 frequency response analyzer in combination with the Solartron 1287 potentiostat was used to determine these two parameters of the cell with the $BaZr_{0.9}Y_{0.1}O_{3-\delta}$ electrolyte by sweeping from 0.1 Hz to 1 MHz with a signal amplitude of 100 mV (an example is shown in **Fig. 11(a)**). However, for the cell with the $BaZr_{0.8}Y_{0.2}O_{3-\delta}$ electrolyte, as shown in **Fig. 11(b)**, we could not determine R_{total} with the same method. Instead, the I-V relationship was monitored by applying a very small D. C. voltage signal (< 1 mV deviating from the open circuit voltage) with the Solartron 1287 potentiostat. If assuming that such small voltage will not influence the polarization resistance of the electrodes significantly, R_{total} can be estimated from the linear I-V relationship (an example is given in **Fig. 11(c)**). With these methods, R_{total} and $R_{electrolyte}$ are determined, enabling the correction of the transport numbers (**Fig. 9(b)**). It can be seen that the corrected transport numbers have larger values than the uncorrected ones. And the transport number of the ionic conduction decreased with the increasing temperature. The corrected transport numbers

of the ionic species ($t_{O^{2-}} + t_{H^+}$), are 0.66, 0.38, 0.24 for $BaZr_{0.9}Y_{0.1}O_{3-\delta}$, and 0.75, 0.52, 0.21 for $BaZr_{0.8}Y_{0.2}O_{3-\delta}$ at 500, 600 and 700 ^oC, respectively, very close to those determined from the variation of total conductivity with the change of partial pressure of oxygen. The detailed values of transport numbers are list in **Table 2**.

3.3 Transport Properties of Ba-deficient Y-Doped $BaZrO_3$

Ignoring the effect from the electrode polarization seems to be the most possible reason for why the transport numbers reported by Schober and Bohn [5] are different from the others [6, 11, 12]. However, since the $BaZr_{0.9}Y_{0.1}O_{3-\delta}$ sample of Schober and Bohn was sintered at a higher temperature (1715 ^oC) for longer time (30 h), and there is no information on whether their sample was buried in a sacrificial powder to prevent the loss of BaO during sintering [5], one may suspect their sample to be quite Ba-deficient [33]. Such Ba-deficiency may also influence the transport property. We thereby studied the effect of Ba-deficiency on the transport property in a 20 mol% Y-doped system, by introducing the Ba-deficiency of 0.02 ($Ba_{0.98}Zr_{0.8}Y_{0.2}O_{3-\delta}$) and 0.05 ($Ba_{0.95}Zr_{0.8}Y_{0.2}O_{3-\delta}$). The results of conductivity measurements, as shown in **Fig. 12**, indicate that with the increasing Ba-deficiency, the bulk, grain boundary and total conductivities all decreased. Such results agree with the previous reports. [30, 35] Then, the EMF method corrected by taking the effect of electrode polarization into consideration was applied to determine the transport numbers (the measured EMFs are given in supplementary material). Almost pure proton conduction occurred in all the three samples in the

reducing atmosphere (**Fig. 13(a)**). And there is no great difference in the transport numbers of the ionic species between stoichiometric and Ba-deficient samples (**Fig. 13(b)**). The detailed values are given in **Table 3**.

3.4 Transport Properties of $BaZrO_3$ Doped with Sc, In, Ho, Er, Tm and Yb

The transport numbers, which are determined by the EMF method with the consideration of the effect of electrode polarization, of $BaZr_{0.8}M_{0.2}O_{3-\delta}$ (M = Sc, In, Ho, Er, Tm and Yb) are given in **Table 4**, and are plotted in **Fig. 14** (the measured EMFs are given in supplementary material). There is no special dependence of the transport property on the dopants in $BaZrO_3$. Regardless of which dopant is introduced into $BaZrO_3$, proton conduction dominates in the reducing atmosphere (**Fig. 14(a)**), and a mixed conduction of protons and holes occurred in the oxidizing atmosphere (**Fig. 14(b)**). However, it can be seen that Y-doped $BaZrO_3$ has a relatively high transport number in the oxidizing atmosphere (circle symbols in **Fig. 14(b)**).

4. Discussion

Almost pure proton conduction is confirmed when the acceptor-doped $BaZrO_3$ is exposed to the moist reducing atmosphere, regardless what kind of dopant or whether Ba-deficiency is introduced. However, when exposing to the oxidizing atmosphere, due to the generation of hole defects, the contribution of ionic conduction decreases, and that of the hole conduction increases. Furthermore,

the contribution of hole conduction is enhanced with the elevating temperature. Although concentrations of protons and holes both decrease with the increasing temperature [7, 36, 37], increment of mobility seems to be much larger for holes than protons. For example, Zhu *et al*. [37] reported that the diffusion coefficient of protons in $BaZr_{0.9}Y_{0.1}O_{3-\delta}$ is 7.46×10^{-11} m^2s^{-1} at 600 ^oC, and nearly doubled (1.84×10^{-10} m^2s^{-1}) at 800 ^oC. However, the diffusion coefficient of holes increases by almost ten times from 1.22×10^{-8} m^2s^{-1} at 600 ^oC to 1.11×10^{-7} m^2S^{-1} at 800 ^oC, resulting in enhanced contribution of hole conduction at elevated temperature. Compared with the conduction of protons and holes, the contribution of that of oxide ions is negligibly small, possibly due to the too low mobility of oxide ions in the BZY lattice [37].

A summarization of the reported transport numbers of ionic species in BZY in the wet oxidizing atmosphere is given in **Table 5**. Except for the results reported by Schober and Bohn [5], all the other transport numbers reported in the pure BZY system range from 0.38 to 0.67 with certain discrepancy. Such discrepancy might be partly due to the difference in the atmosphere for measurement. For example, the transport number reported by Kuz'min et al [38] is around 0.67 for $BaZr_{0.9}Y_{0.1}O_{3-\delta}$ in moist air, but smaller values are obtained by Zhu [37] (~ 0.5) and this work (0.38) in moist oxygen atmosphere. Such difference is considered to be due to the decreased contribution of ionic conduction with the increasing partial pressure of oxygen. In **Table 5**, the transport numbers of the system incorporated with Ni, Co and Cu are also listed for comparison. In general, incorporating these metals does not change the transport properties in the reducing atmosphere, and proton conduction still

predominates [40-43]. But, in the oxidizing atmosphere, the contribution of hole conduction increases. For example, Kim *et al*. [12] found that by adding 1 wt% NiO into $BaZr_{0.9}Y_{0.1}O_{3-\delta}$, the contribution of hole conduction was enhanced significantly. In addition, it is worth to note that, in addition to the change in the transport number, incorporating Ni into the BZY also results the electrical conductivity to be greatly degraded. [34, 44, 45] Since NiO is commonly used as sintering aids for BZY, [46, 47] attention should be paid on their deteriorated influence on the transport properties.

5. Conclusions

In this work, a systematic work has been performed to investigate the transport properties of $BaZrO_3$ with various dopants or different Ba-deficiency using the EMF method. The transport numbers of the ionic species (protons and oxide ions) in the oxidizing atmosphere were corrected by taking the effect of electrode polarization into consideration. The results revealed that regardless of whether Sc, Y, In, Ho, Er, Tm or Yb was doped, proton conduction predominates in the reducing atmosphere with the transport number close to unit. However, the contribution of ionic conduction weakens, but the contribution of hole conduction enhances, when the samples are exposed to the moist oxidizing atmosphere. In addition, introducing Ba-deficiency results in degraded electrochemical conductivity, but the transport number in either the moist reducing or the moist oxidizing atmosphere does not change obviously.

Acknowledgement

A part of this study was supported by the New Energy and Industrial Technology Development Organization (NEDO) in Japan (project code P08023).

References

1. Guo Y, Lin Y, Ran R, Shao Z. Zirconium doping effect on the performance of proton-conducting $BaZr_yCe_{0.8-y}Y_{0.2}O_{3-\delta}$ ($0.0 \leq y \leq 0.8$) for fuel cell applications. J Power Sources 2009; 193: 400 - 407.

2. Okumura Y, Nose Y, Katayama J, Uda T. High performance protonic ceramic fuel cells with acid-etched surfaces. J Electhochem Soc 2011; 158: B1067 – B1071.

3. Duan C, Tong J, Shang M, Nikodemski S, Sanders M, Ricote S, Almansoori A, O'Hayer R. Readily processed protonic ceramic fuel cells with high performance at low temperature. Science 2015; 349: 1321 – 1326.

4. Bi L, Shafi SP, Traversa E. Y-doped $BaZrO_3$ as a chemically stable electrolyte for proton-conducting solid oxide electrolysis cells. J Mater Chem A 2015; 3: 5815 – 5819.

5. Schober T, Bohn HG. Water vapour solubility and electrochemical characterization of the high temperature proton conductor $BaZr_{0.9}Y_{0.1}O_{3-\delta}$. Solid State Ionics 2000; 127: 351 - 360.

6. Nomura K, Kageyama H. Transport properties of $Ba(Zr_{0.8}Y_{0.2})O_{3-\delta}$ perovskite. Solid State Ionics 2007; 178: 661 – 665.

7. Han D, Nose Y, Shinoda K, Uda T. Site selectivity of dopants in $BaZr_{1-y}M_yO_{3-\delta}$ (M = Sc, Y, Sm, Eu,

Dy) and measurement of their water contents and conductivities. Solid State Ionics 2012; 213: 2 – 7.

8. Han D, Shinoda K, Sato S, Majima M, Uda T. Correlation between Electroconductive and structural properties of proton conductive acceptor-doped barium zirconate. J Mater Chem A 2015; 3: 1243 – 1250.

9. Han D, Hatada N, M, Uda T. Chemical expansion of yttrium-doped barium zirconate and correlation with proton concentration and conductivity. J Am Ceram Soc 2016; doi: 10.1111/jace.14377.

10. Lai W, Haile SM. Electrochemical impedance of mixed conductors under a chemical potential gradient: a case study of Pt|SDC|BSCF. Phys Chem Chem Phys 2008; 10: 865-883.

11. Wang W, Virkar AV. Ionic and electron-hole conduction in $BaZr_{0.93}Y_{0.07}O_{3-\delta}$ by 4-probe dc measurements. J Power Sources 2005; 142: 1-9.

12. Kim E, Yamazaki Y, Haile SM, Yoo HI. Effect of NiO sintering-aid on hydration kinetics and defect-chemical parameters of $BaZr_{0.8}Y_{0.2}O_{3-\triangle}$. Solid State Ionics 2015; 275: 23-28.

13. Imashuku S, Uda T, Nose Y, Taniguchi G, Ito Y, Awakura Y. Dependence of dopants cations on microstructure and proton conductivity of barium zirconate. J Electrochem Soc 2009; 156: B1 – B8.

14. Han D, Hatada N, Uda T. Microstructure, proton concentration and proton conductivity of barium zirconate doped with Ho, Er, Tm and Yb. J Electrochem Soc 2016; 163: F470-476.

15. Norby T. EMF method determination of conductivity contributions from protons and other foreign

ions in oxides. Solid State Ionics 1988; 28 – 30: 1586 – 1591.

16. Fujii H, Katayama Y, Shimura T, Iwahara H. Protonic conduction in perovskite-type oxide ceramics based on $LnScO_3$ (Ln = La, Nd, Sm or Gd) at high temperature. J Elecroceram 1998; 2: 119 – 125.

17. Shimura T, Fujimoto S, Iwahara H. Proton conduction in non-perovskite-type oxides at elevated temperatures. Solid State Ionics 2001; 143: 117 – 123.

18. Shimura T, Esaka K, Matsumoto H, Iwahara H. Protonic conduction in Rh-doped $AZrO_3$ (A = Ba, Sr and Ca). Solid State Ionics 2002; 149: 237 – 246.

19. Ma G, Zhang F, Zhu J, Meng G. Proton conduction in $La_{0.9}Sr_{0.1}Ga_{0.8}Mg_{0.2}O_{3-\delta}$. Chem Mater 2006; 18: 6006 – 6011.

20. Ricote S, Bonanos N, Wang HJ, Haugsrud R. Conductivity, transport number measurements and hydration thermodynamics of $BaCe_{0.2}Zr_{0.7}Y_{(0.1-\xi)}Ni_{\xi}O_{(3-\delta)}$. Solid State Ionics 2011; 185: 11 – 17.

21. Li L, Nino JC. Proton-conducting barium stannates: doping strategies and transport properties. Int J Hydrogen Energ 2013; 38: 1598 – 1606.

22. Kreuer KD. Proton-conducting oxides. Annu Rev Mater Res 2003; 33: 333-359.

23. Lybye D, Bonanos N. Proton and oxide ion conductivity of doped $LaScO_3$. Solid State Ionics 1999; 125: 339-344.

24. Bonanos N. Oxide-based protonic conductors: point defects and transport properties. Solid State Ionics 2001; 145: 265-274.

25. Liu M, Hu H. Effect of interfacial resistance on determination of transport properties of mixed-conducting electrolytes. J Electrochem Soc 1996; 143: L109-L112.

26. Kharton VV, Marques FMB. Interfacial effects in electrochemical cells for oxygen ionic conduction measurements I. The e.m.f. method. Solid State Ionics 2001; 140: 381-394.

27. Bentzer HK, Bonanos N, Phair JW. EMF measurements on mixed protonic/electronic conductors for hydrogen membrane applications. Solid State Ionics 2010; 181: 249-255.

28. Pérez-Coll D, Heras-Juaristi G, Fagg, DP, Mather GC. Transport-number determination of a protonic ceramic electrolyte membrane via electrode-polarization correction with the Gorelov method. J Power Sources 2014; 245: 445-455.

29. Pérez-Coll D, Heras-Juaristi G, Fagg, DP, Mather GC. Methodology for the study of mixed transport properties of a Zn-doped $SrZr_{0.9}Y_{0.1}O_{3-\delta}$ electrolyte under reducing conditions. J Mater Chem A 2015; 3: 11098-11110.

30. Yamazaki Y, Hernandez-Sanchez R, Haile SM. Cation non-stoichiometry in yttrium-doped baium zirconate: phase behavior, microstructure, and proton conductivity. J Mater Chem 2010; 20: 8158 – 8166.

31. Han D, Kishida K, Shinoda K, Haruyuki I, Uda T. A comprehensive understanding of structure and site occupancy of Y in Y-doped $BaZrO_3$. J Mater Chem A 2013; 1: 3027-3033.

32. Han D, Shinoda K, Uda T. Dopant site occupancy and chemical expansion in rare earth-doped barium zirconate. J Am Ceram Soc 2014; 97: 643-650.

33. Babilo P, Uda T, Haile SM. Processing of yttrium-doped barium zirconate for high proton conductivity. J Mater Res 2007; 22: 1322 – 1330.

34. Han D, Iihara J, Uemura S, Kazumi K, Hiraiwa C, Majima M, Uda T. A high temperature reduction cleaning (HTRC) process: a novel method for conductivity recovery of yttrium-doped barium zirconate electrolytes. J Mater Chem A 2016; 4: 10601-10608.

35. Han D, Kishida K, Inui H, Uda T. Substantial appearance of origin of conductivity decrease in Y-doped $BaZrO_3$ due to Ba-deficiency. RSC Adv 2014; 4: 31589 – 31593.

36. Kreuer KD. Aspects of the formation and mobility of protonic charge carriers and the stability of perovskite-type oxide. Solid State Ionics 1999; 125: 285-302.

37. Zhu H, Ricote S, Grover Coors W, Kee RJ. Interpreting equilibrium-conductivity and conductivity-relaxation measurements to establish thermodynamic and transport properties for multiple charged defect conducting creamics. Faraday Discuss 2015; 182: 49-74.

38. Kuz'min AV, Balakireva VB, Plaksin SV, Gorelov VP. Total and hole conductivity in the $BaZr_{1-x}Y_xO_{3-\alpha}$ system (x = 0.02-0.20) in oxidizing atmosphere. Rus J Electrochem 2009; 45: 1351-1357.

39. Gorelov VP, Balakireva VB, Kuz'min AV. Ionic, proton and oxygen conductivities in the $BaZr_{1-x}Y_xO_{3-\alpha}$ system (x = 0.02-0.15) in humid air. Rus J Electrochem 2010; 46: 890-895.

40. Choi SM, Lee J, Ji HL, Yoon KJ, Son J, Kim B, Je HJ, Lee H, Lee J. Determination of proton transference number of $Ba(Zr_{0.84}Y_{0.15}Cu_{0.01})O_{3-\delta}$ via electrochemical concentration cell test. J Solid State Electrochem 2013; 17: 2833-2838.

41. Azimova MA, McIntosh S. Transport properties and stability of cobalt doped proton conducting oxides. Solid State Ionics 2009; 180: 160-167.

42. Ricote S, Bonanos N, Wang H, Haugsrud R. Conductivity, transport number measurements and hydration thermodynamics of $BaCe_{0.2}Zr_{0.7}Y_{(0.1-\xi)}Ni_{\xi}O_{(3-\delta)}$. Solid State Ionics 2011; 185: 11-17.

43. Babilo P, Haile SM. Enhanced sintering of yttrium-doped barium zirconate by addition of ZnO. J Am Ceram Soc 2005; 88: 2362-2368.

44. Han D, Shinoda K, Tsukimoto S, Takeuchi H, Hiraiwa C, Majima M, Uda T. Origins or structural and electrochemical influence on Y-doped $BaZrO_3$ heat-treated with NiO additive. J Mater Chem A 2014; 2: 12552-12560.

45. Polfus JM, Fontaine M, Thøgersen A, Riktor M, Norby T, Bredesen R. Solubility of transition metal interstitials in proton conducting $BaZrO_3$ and similar perovskite oxides. J Mater Chem A 2016; 4: 8105-8112.

46. Tong J, Clark D, Bernau L, Sanders M, O'Hayre. Solid-state reactive sintering mechanism for large-grained yttrium-doped barium zirconate proton conducting ceramics. J Mater Chem 2010; 20: 6333-6341.

47. Nikodemski S, Tong J, O'Hayre, Solid-state reactive sintering mechanism for proton conducting ceramics. Solid State Ionics 2013; 253: 201-210.

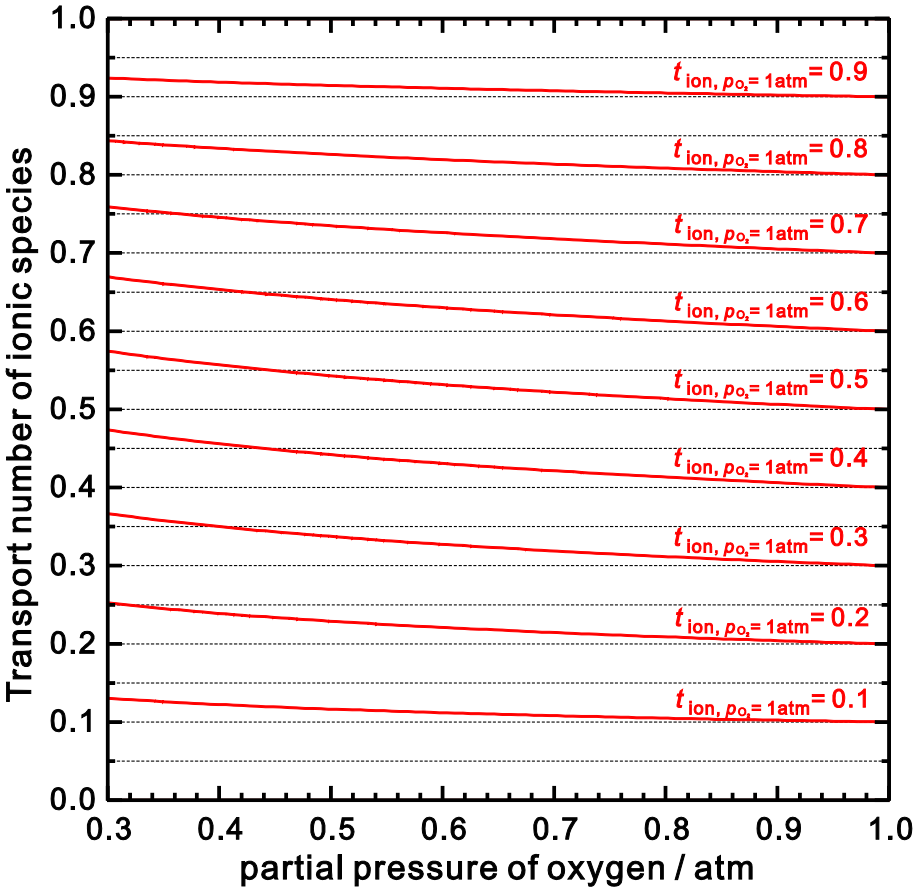

Fig. 1 Simulated transport numbers of ionic species (oxide ions and protons) in oxidizing atmosphere. The curves are drawn by assuming that the transport numbers of the ionic species at the partial pressure of oxygen of 1 atm range from 0.1 to 0.9.

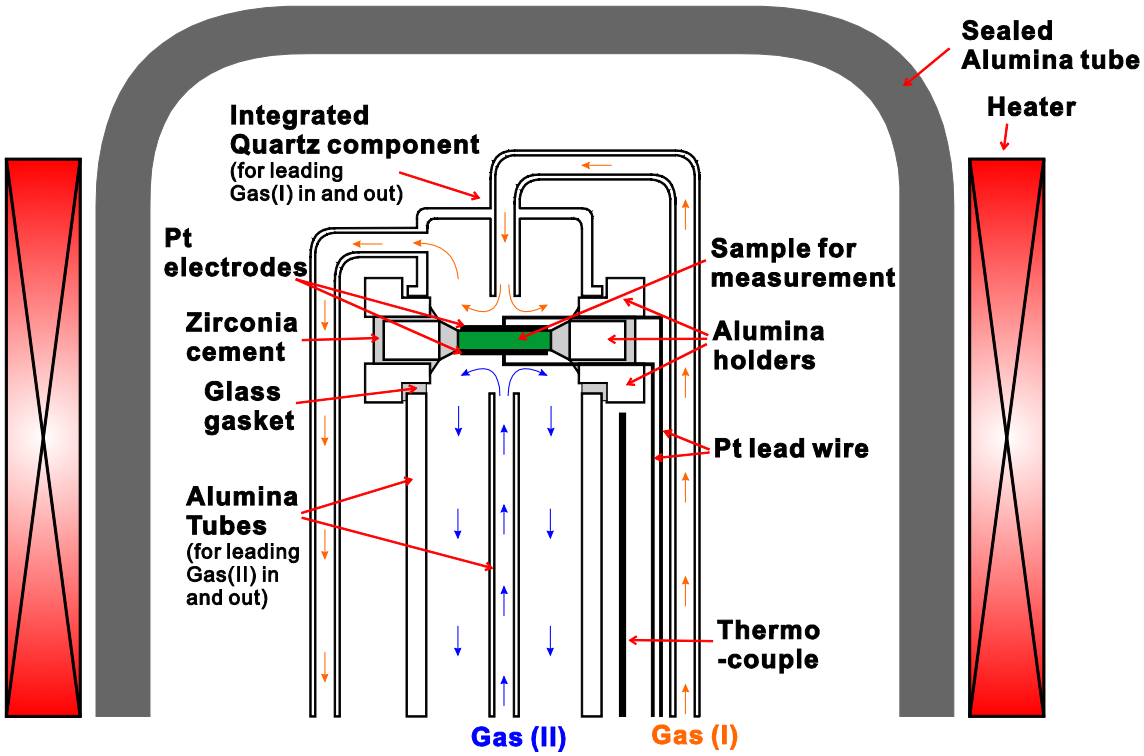

Fig. 2 A schematic of device and sample setting for EMF measurement.

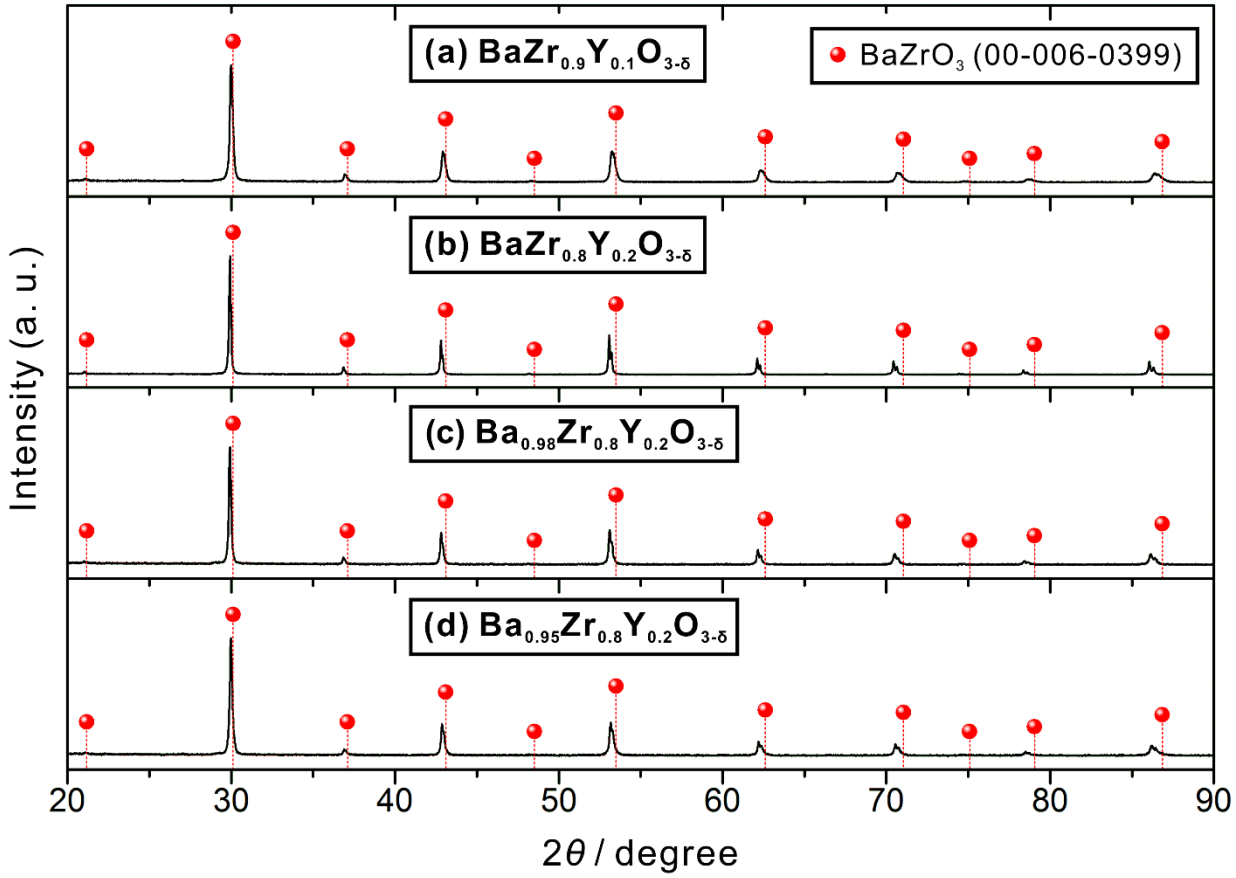

Fig. 3 Powder XRD patterns of (a) $BaZr_{0.9}Y_{0.1}O_{3-\delta}$, (b) $BaZr_{0.8}Y_{0.2}O_{3-\delta}$, (c) $Ba_{0.98}Zr_{0.8}Y_{0.2}O_{3-\delta}$ and (d) $Ba_{0.95}Zr_{0.8}Y_{0.2}O_{3-\delta}$. All the samples were sintered at 1600 ^{o}C in O_2 for 24 h.

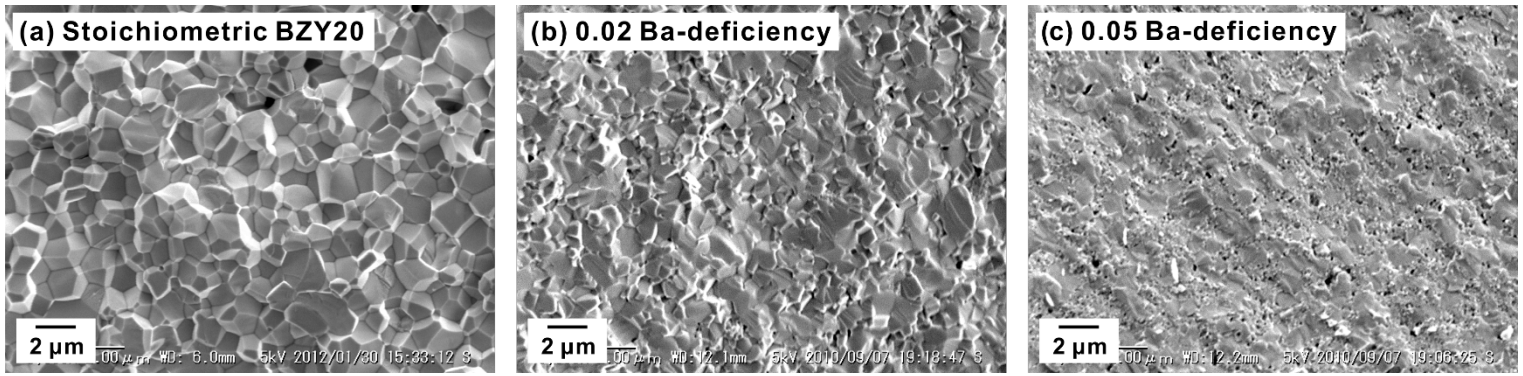

Fig. 4 SEM image of fractured cross-section of (a) stoichiometric $BaZr_{0.8}Y_{0.2}O_{3-\delta}$ [9], (b) $Ba_{0.98}Zr_{0.8}Y_{0.2}O_{3-\delta}$, and (c) $Ba_{0.95}Zr_{0.8}Y_{0.2}O_{3-\delta}$. All the samples were finally sintered at 1600 ^{o}C in O_2 for 24 h.

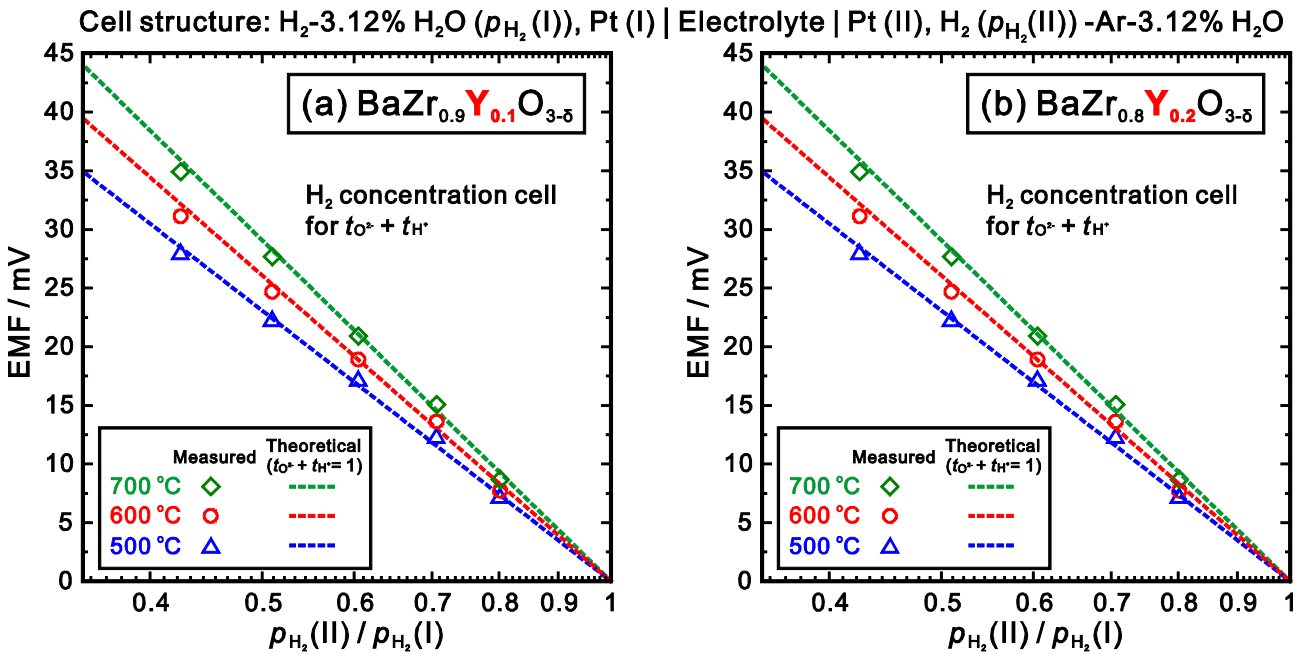

Fig. 5 EMF values of hydrogen concentration cells (Cell 1) using (a) $BaZr_{0.9}Y_{0.1}O_{3-\delta}$, and (b) $BaZr_{0.8}Y_{0.2}O_{3-\delta}$ as the electrolytes at 500, 600 and 700 ^{o}C, plotted against the ratio of partial pressure of hydrogen at electrodes (II) and (I). Identical p_{H_2O} of 0.0312 atm was maintained at both the two electrodes.

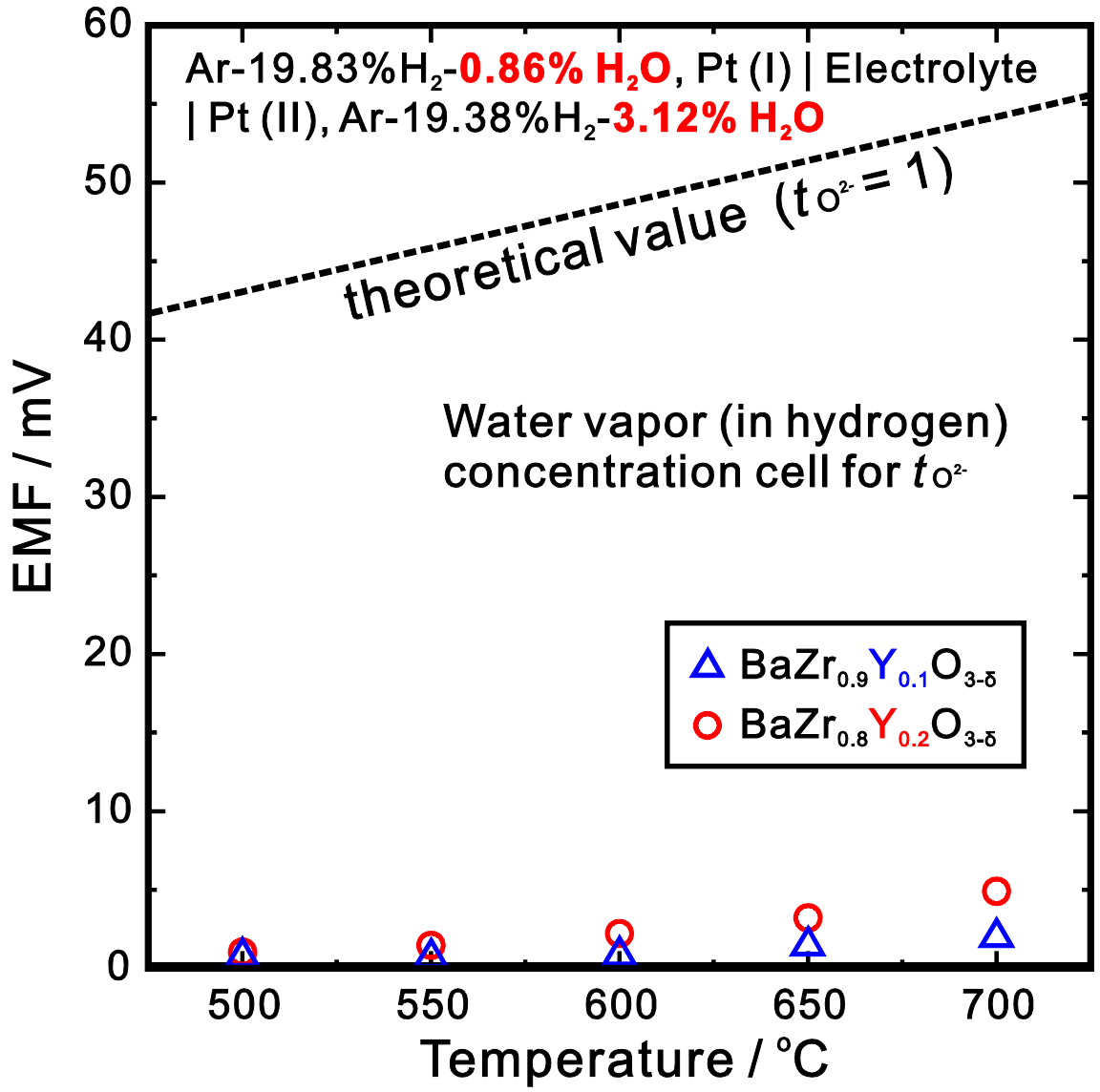

Fig. 6 EMF values of water vapor (in hydrogen) concentration cells (Cell 2) using $BaZr_{0.9}Y_{0.1}O_{3-\delta}$ and $BaZr_{0.8}Y_{0.2}O_{3-\delta}$ as the electrolytes between 500 and 700 °C with an interval of 50 °C. p_{H_2O} was 0.0086 and 0.0312 atm in the atmospheres at the electrode (I) and (II), respectively.

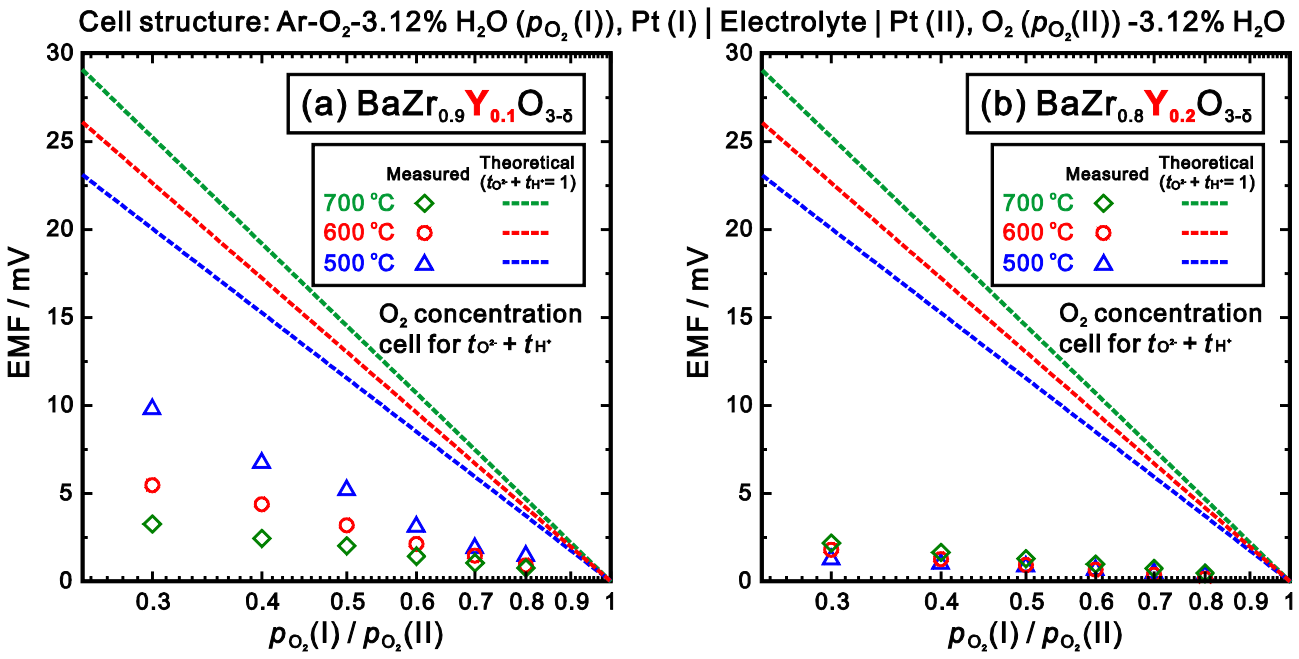

Fig. 7 EMF values of oxygen concentration cells (Cell 3) using (a) $BaZr_{0.9}Y_{0.1}O_{3-\delta}$, and (b) $BaZr_{0.8}Y_{0.2}O_{3-\delta}$ as the electrolytes at 500, 600 and 700 ^{o}C, plotted against the ratio of partial pressure of oxygen at electrodes (I) and (II). Identical p_{H_2O} of 0.0312 atm was maintained at both the two electrodes.

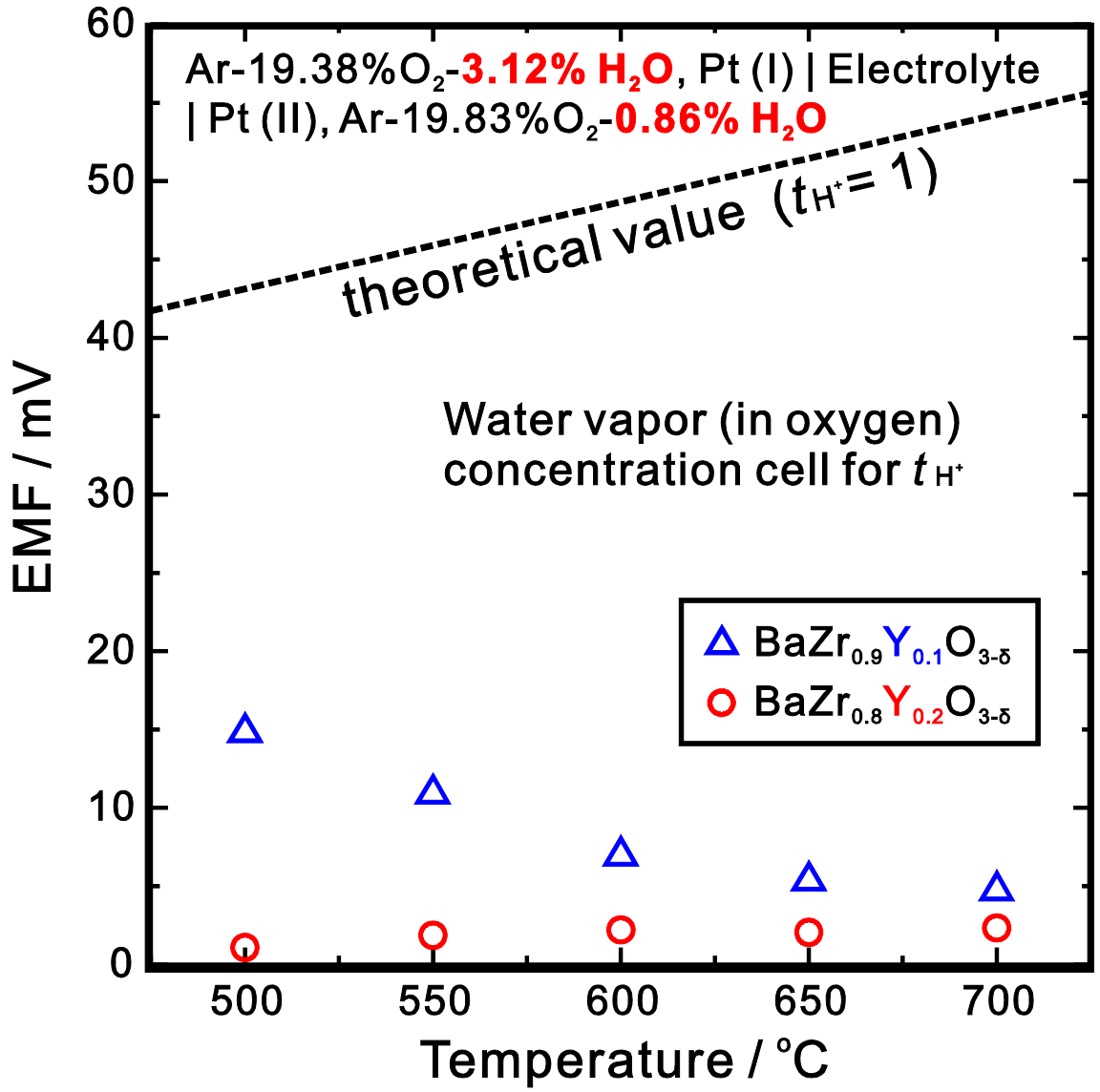

Fig. 8 EMF values of water vapor (in oxygen) concentration cells (Cell 4) using $BaZr_{0.9}Y_{0.1}O_{3-\delta}$ and $BaZr_{0.8}Y_{0.2}O_{3-\delta}$ as the electrolytes between 500 and 700 °C with an interval of 50 °C. p_{H_2O} was 0.0312 and 0.0086 atm in the atmospheres at the electrode (I) and (II), respectively.

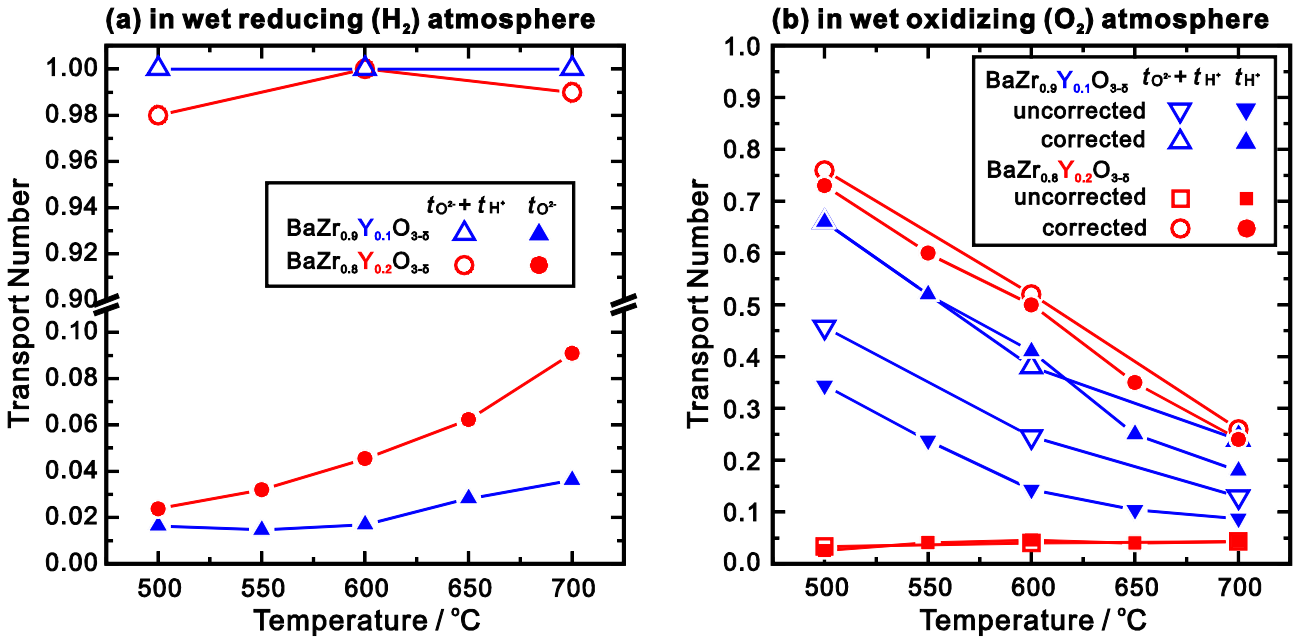

Fig. 9 Transport numbers of $BaZr_{0.9}Y_{0.1}O_{3-\delta}$ and $BaZr_{0.8}Y_{0.2}O_{3-\delta}$ in (a) H_2-contained reducing atmosphere, and (b) O_2-contained oxidizing atmosphere in this work. The results of $t_{O^{2-}} + t_{H^+}$ and $t_{O^{2-}}$ in (a) were measured by hydrogen concentration cells (Cell 1) and water vapor (in hydrogen) concentration cells (Cell 2), respectively. And the results of $t_{O^{2-}} + t_{H^+}$ and t_{H^+} were measured by oxygen concentration cells (Cell 3) and water vapor (in oxygen) concentration cells (Cell 4), respectively. Both the uncorrected (simply dividing the measured EMF value with the theoretical ones) and corrected values (by taking the electrode polarization into consideration) are shown for the case in wet oxidizing atmosphere.

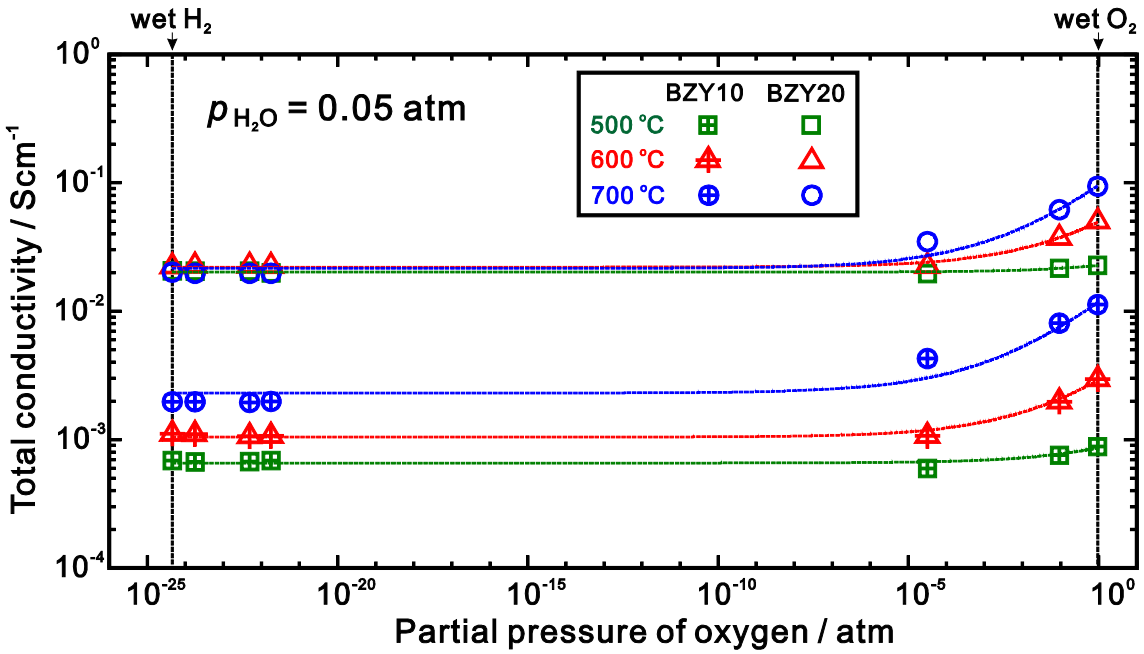

Fig. 10 Dependence of total conductivity of $BaZr_{0.9}Y_{0.1}O_{3-\delta}$ (BZY10) and $BaZr_{0.8}Y_{0.2}O_{3-\delta}$ (BZY20) on partial pressure of oxygen. The oxygen partial pressure was controlled by mixing Ar with hydrogen or oxygen. The partial pressure of water vapor was kept as 0.05 atm. Dash lines are the fitting results using Eq. (7).

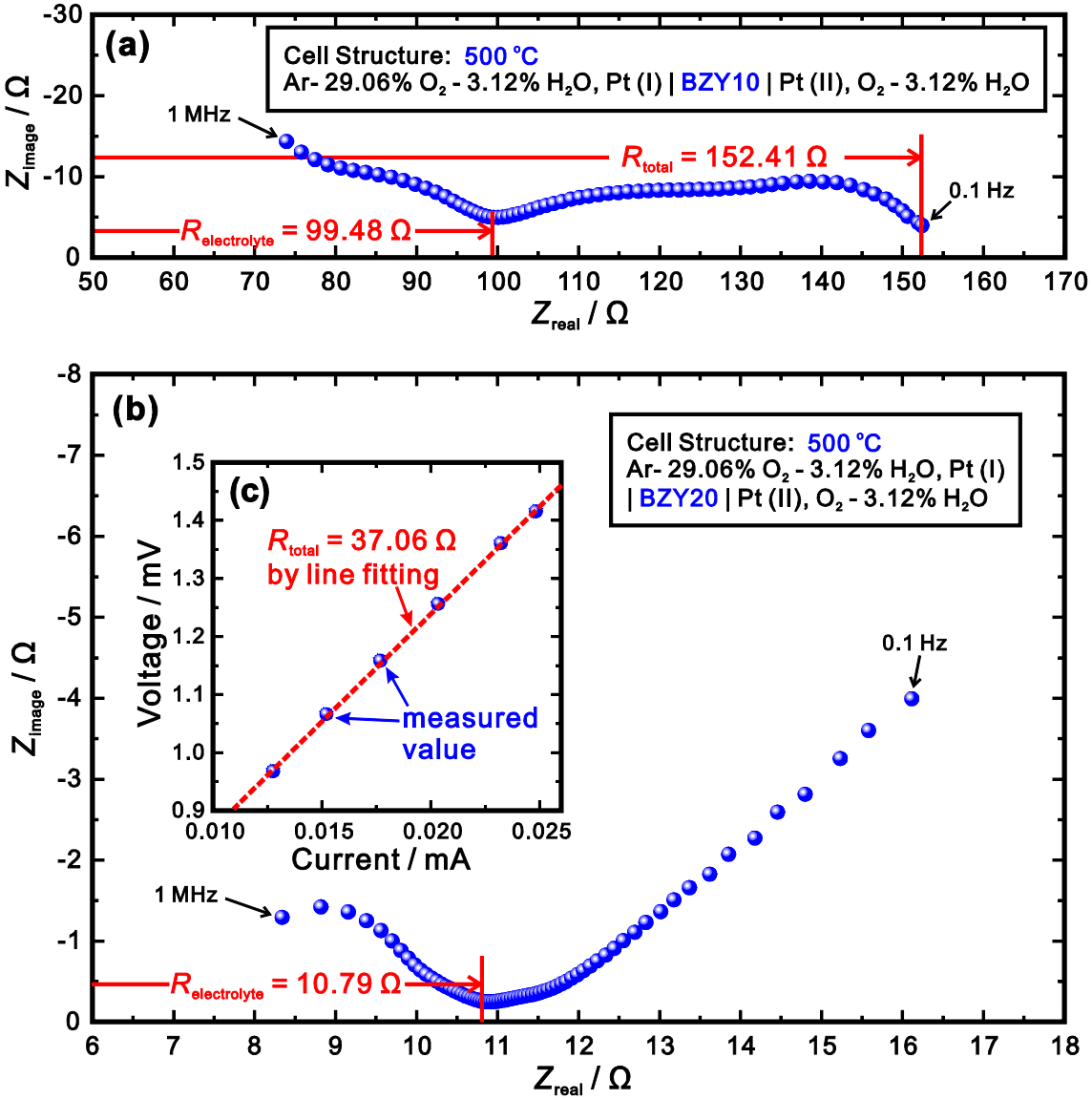

Fig. 11 Impedance spectra of (a) $BaZr_{0.9}Y_{0.1}O_{3-\delta}$ (BZY10) and (b) $BaZr_{0.8}Y_{0.2}O_{3-\delta}$ (BZY20), and (c) I-V relationship of BZY20 at 500 °C in the mode of oxygen concentration cell by feeding gases of Ar – 29.06% O_2 - 3.12% H_2O and O_2 – 3.12% H_2O to the two electrodes.

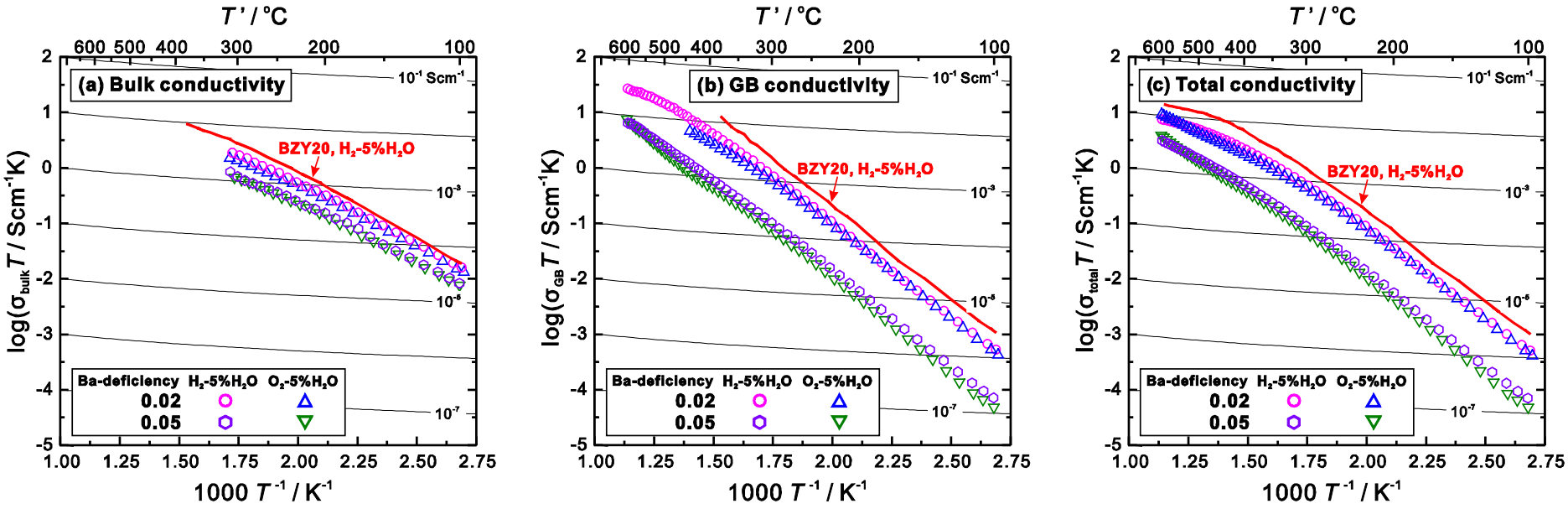

Fig. 12 Arrhenius plots of (a) bulk conductivity, (b) grain boundary conductivity, and (c) total conductivity of 20 mol% Y-doped $BaZrO_3$ with Ba deficiency of 0.02 and 0.05 in wet H_2 or O_2 atmosphere with partial pressure of water vapor of 0.05 atm. The conductivity of stoichiometric $BaZr_{0.8}Y_{0.2}O_{3-\delta}$ [34] in wet H_2 is also plotted for comparison. The samples for conductivity measurement were finally sintered at 1600 °C in O_2 for 24 h.

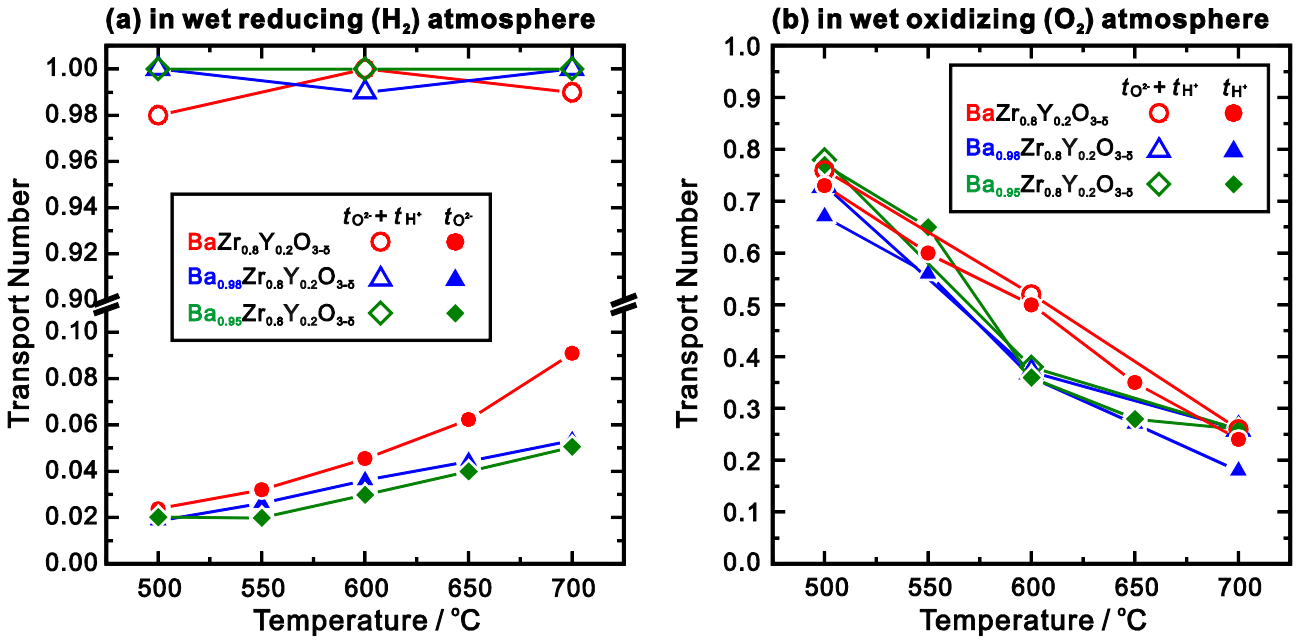

Fig. 13 Transport numbers of $Ba_{0.98}Zr_{0.8}Y_{0.2}O_{3-\delta}$ and $Ba_{0.95}Zr_{0.8}Y_{0.2}O_{3-\delta}$ in (a) H_2-contained reducing atmosphere, and (b) O_2-contained oxidizing atmosphere in this work. The results of $t_{O^{2-}} + t_{H^+}$ and $t_{O^{2-}}$ in (a) were measured by hydrogen concentration cells (Cell 1) and water vapor (in hydrogen) concentration cells (Cell 2), respectively. And the results of $t_{O^{2-}} + t_{H^+}$ and t_{H^+} were measured by oxygen concentration cells (Cell 3) and water vapor (in oxygen) concentration cells (Cell 4), respectively, and compensated by taking the effect from electrode polarization into consideration.

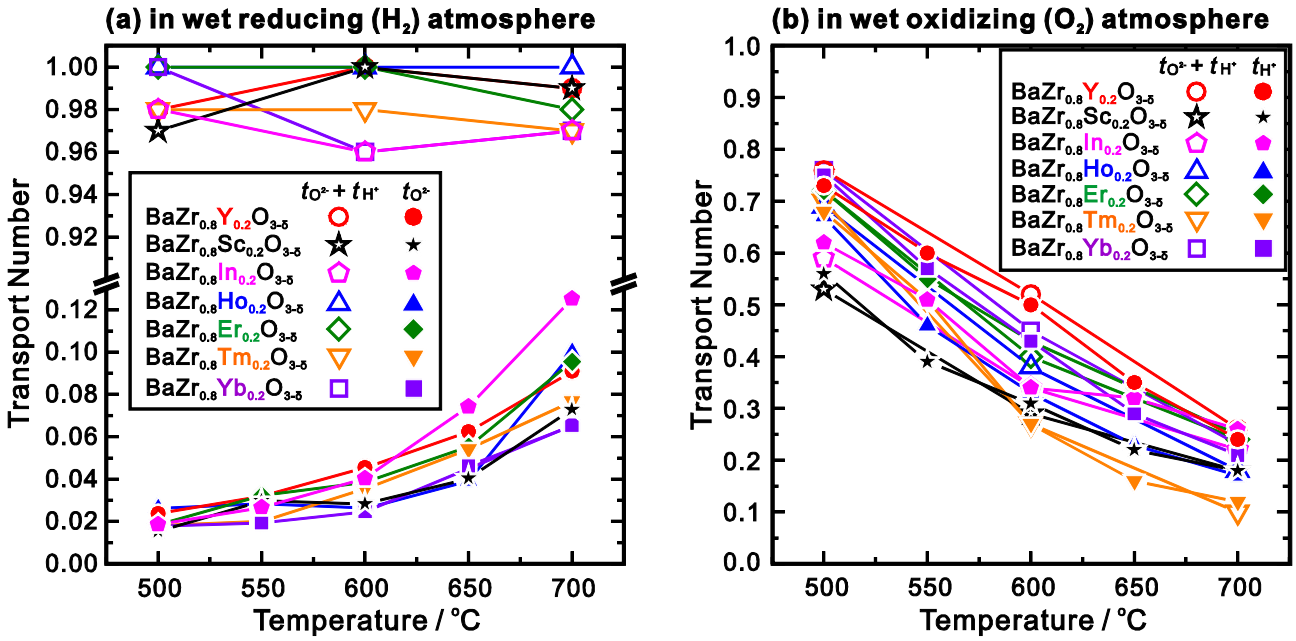

Fig. 14 Transport numbers of $BaZr_{0.8}M_{0.2}O_{3-\delta}$ (M = Sc, In, Y, Ho, Er, Tm and Yb) as the electrolytes in (a) H_2-contained reducing atmosphere, and (b) O_2-contained oxidizing atmosphere in this work. The results of $t_{O^{2-}} + t_{H^+}$ and $t_{O^{2-}}$ in (a) were measured by hydrogen concentration cells (Cell 1) and water vapor (in hydrogen) concentration cells (Cell 2), respectively. And the results of $t_{O^{2-}} + t_{H^+}$ and t_{H^+} were measured by oxygen concentration cells (Cell 3) and water vapor (in oxygen) concentration cells (Cell 4), respectively, and compensated by taking the effect from electrode polarization into consideration

Table 1 Total composition determined by ICP-AES. All the samples were finally heat-treated at 1600 ^{o}C in O_2 for 24 h for sintering.

Nominal Composition	Actual Composition by ICP-AES
$BaZr_{0.9}Y_{0.1}O_{3-\delta}$	$Ba_{1.00}Zr_{0.90}Y_{0.10}O_{3-\delta}$
$BaZr_{0.8}Y_{0.2}O_{3-\delta}$	$Ba_{0.99}Zr_{0.81}Y_{0.19}O_{3-\delta}$
$Ba_{0.98}Zr_{0.8}Y_{0.2}O_{3-\delta}$	$Ba_{0.98}Zr_{0.78}Y_{0.22}O_{3-\delta}$
$Ba_{0.95}Zr_{0.8}Y_{0.2}O_{3-\delta}$	$Ba_{0.95}Zr_{0.80}Y_{0.20}O_{3-\delta}$

Table 2 Transport numbers of stoichiometric $BaZr_{0.9}Y_{0.1}O_{3-\delta}$, $BaZr_{0.8}Y_{0.2}O_{3-\delta}$.

Composition	Temperature / °C	H_2-contained reducing atmosphere		O_2-contained oxidizing atmosphere				
		$t_{H^+} + t_{O^{2-}}$	$t_{O^{2-}}$	$t_{H^+} + t_{O^{2-}}$			t_{H^+}	
				Conductivity measurements	EMF measurements		EMF measurements	
					uncorrected	corrected	uncorrected	corrected
$BaZr_{0.9}Y_{0.1}O_{3-\delta}$	500	1.00	0.016	0.76	0.46	0.66	0.35	0.67
	550		0.015				0.24	0.52
	600	1.00	0.017	0.36	0.25	0.38	0.14	0.41
	650		0.028				0.10	0.25
	700	1.00	0.036	0.20	0.13	0.24	0.087	0.18
$BaZr_{0.8}Y_{0.2}O_{3-\delta}$	500	0.98	0.024	0.89	0.033	0.75	0.026	0.73
	550		0.032				0.041	0.60
	600	1.00	0.046	0.45	0.040	0.52	0.046	0.50
	650		0.062				0.040	0.35
	700	0.99	0.091	0.23	0.043	0.26	0.043	0.24

Table 3 Transport numbers of Ba-deficient $Ba_{0.98}Zr_{0.8}Y_{0.2}O_{3-\delta}$, $Ba_{0.95}Zr_{0.8}Y_{0.2}O_{3-\delta}$ determined by electromotive force measurements

Composition	Temperature / °C	H_2-contained reducing atmosphere		O_2-contained oxidizing atmosphere			
		$t_{H^+} + t_{O^{2-}}$	$t_{O^{2-}}$	$t_{H^+} + t_{O^{2-}}$		t_{H^+}	
				uncorrected	corrected	uncorrected	corrected
$Ba_{0.98}Zr_{0.8}Y_{0.2}O_{3-\delta}$	500	1.00	0.019	0.25	0.73	0.14	0.67
	550		0.026			0.15	0.60
	600	0.99	0.036	0.16	0.37	0.14	0.36
	650		0.044			0.12	0.27
	700	1.00	0.053	0.13	0.26	0.098	0.18
$Ba_{0.95}Zr_{0.8}Y_{0.2}O_{3-\delta}$	500	1.00	0.020	0.093	0.78	0.059	0.77
	550		0.020			0.062	0.65
	600	1.00	0.030	0.12	0.38	0.078	0.36
	650		0.040			0.078	0.26
	700	1.00	0.051	0.11	0.25	0.066	0.28

Table 4 Transport numbers of stoichiometric $BaZr_{0.8}M_{0.2}O_{3-\delta}$ (M = Sc, In, Ho, Er, Tm and Yb) determined by electromotive force measurements.

Composition	Temperature / °C	H_2-contained reducing atmosphere		O_2-contained oxidizing atmosphere			
		$t_{H^+} + t_{O^{2-}}$	$t_{O^{2-}}$	$t_{H^+} + t_{O^{2-}}$		t_{H^+}	
				uncorrected	corrected	uncorrected	corrected
$BaZr_{0.8}Sc_{0.2}O_{3-\delta}$	500	0.97	0.015	0.020	0.53	0.027	0.56
	550		0.030			0.031	0.39
	600	1.00	0.028	0.033	0.29	0.032	0.31
	650		0.041			0.033	0.22
	700	0.99	0.073	0.042	0.18	0.036	0.18
$BaZr_{0.8}In_{0.2}O_{3-\delta}$	500	0.98	0.019	0.11	0.59	0.078	0.62
	550		0.027			0.092	0.51
	600	0.96	0.041	0.081	0.34	0.080	0.34
	650		0.074			0.051	0.32
	700	0.97	0.13	0.062	0.22	0.048	0.26
$BaZr_{0.8}Ho_{0.2}O_{3-\delta}$	500	1.00	0.026	0.029	0.69	0.019	0.67
	550		0.029			0.028	0.46
	600	1.00	0.026	0.048	0.38	0.032	0.33
	650		0.039			0.034	0.23
	700	1.00	0.10	0.056	0.18	0.038	0.17
$BaZr_{0.8}Er_{0.2}O_{3-\delta}$	500	1.00	0.019	0.042	0.72	0.026	0.72
	550		0.032			0.030	0.55
	600	1.00	0.039	0.050	0.40	0.043	0.43
	650		0.055			0.045	0.34
	700	0.98	0.096	0.073	0.24	0.041	0.25
$BaZr_{0.8}Tm_{0.2}O_{3-\delta}$	500	0.98	0.018	0.036	0.70	0.019	0.68
	550		0.020			0.031	0.51
	600	0.98	0.036	0.070	0.27	0.047	0.27
	650		0.054			0.043	0.16
	700	0.97	0.077	0.057	0.10	0.044	0.12
$BaZr_{0.8}Yb_{0.2}O_{3-\delta}$	500	1.00	0.018	0.037	0.76	0.022	0.75
	550		0.019			0.030	0.57
	600	0.96	0.025	0.065	0.45	0.051	0.43
	650		0.046			0.058	0.29
	700	0.97	0.066	0.075	0.23	0.060	0.21

Table 5 Reported $t_{H^+} + t_{O^{2-}}$ in wet oxidizing atmosphere at 600 °C. Temperature other than 600 °C are listed in the brackets.

Reporter	Electrolyte composition	$t_{H^+} + t_{O^{2-}}$	Atmosphere		Method
			p_{O_2} / atm	p_{H_2O} / atm	
Schober [5]	$BaZr_{0.9}Y_{0.1}O_{3-\delta}$	~ 0.07	~ 0.02	0.023	EMF method
Nomura [6]	$BaZr_{0.8}Y_{0.2}O_{3-\delta}$	0.4	0.96	0.042	Dependence of conductivity on p_{O_2}
Wang [11]	$BaZr_{0.93}Y_{0.07}O_{3-\delta}$	> 0.5 (t_{H^+} at 500 °C)	0.2	0.025	Conductivity measurement
Kuz'min [38]	$BaZr_{0.9}Y_{0.1}O_{3-\delta}$	~ 0.67	0.2	0.03	Conductivity measurement
Gorelov [39]	$BaZr_{0.98}Y_{0.2}O_{3-\delta}$ $BaZr_{0.85}Y_{0.15}O_{3-\delta}$	~ 0.5 ~ 0.6	0.2	0.035	Conductivity measurement
Zhu [37]	$BaZr_{0.9}Y_{0.1}O_{3-\delta}$	~ 0.5	0.96	0.038	Dependence of conductivity on p_{O_2}
Choi [40]	$BaZr_{0.84}Y_{0.15}Cu_{0.01}O_{3-\delta}$	0.234 (t_{H^+} at 650 °C)	0.2	0.03	EMF method
Azimova [41]	$BaCe_{0.5}Zr_{0.4}Yb_{0.07}Co_{0.03}O_{3-\delta}$	0.07 (500 °C) 0.03 (700 °C)	> 0.073	0.03	EMF methods
Ricote [42]	$BaCe_{0.2}Zr_{0.7}Y_{0.19}Ni_{0.01}O_{3-\delta}$ $BaCe_{0.2}Zr_{0.7}Y_{0.18}Ni_{0.02}O_{3-\delta}$	0.28 0.25	0.97	0.03	Dependence of conductivity on p_{O_2}
Kim [12]	$BaZr_{0.8}Y_{0.2}O_{3-\delta}$ $BaZr_{0.8}Y_{0.2}O_{3-\delta}$–1 wt% NiO	~ 0.2 (700 °C) < 0.1 (700 °C)	0.99	0.01	Conductivity relaxation
This work	$BaZr_{0.9}Y_{0.1}O_{3-\delta}$ $BaZr_{0.8}Y_{0.2}O_{3-\delta}$	0.38 0.52	0.97	0.0312	EMF method corrected with electrode polarization